ACS SENSORS

pubs.acs.org/acssensors

Article

Molecule-Specific Terahertz Biosensors Based on an Aptamer Hydrogel-Functionalized Metamaterial for Sensitive Assays in Aqueous Environments

Jie Zhou,[‖] Xiang Zhao,*[,‖] Guorong Huang, Xiang Yang, Yang Zhang, Xinyu Zhan, Huiyan Tian, Yu Xiong, Yunxia Wang,* and Weiling Fu*

Cite This: *ACS Sens.* 2021, 6, 1884–1890

Read Online

ACCESS | Metrics & More | Article Recommendations | Supporting Information

ABSTRACT: Metamaterial-inspired terahertz (THz) biosensors are devoted to developing high-sensitivity and label-free biosensing strategies. However, most meaningful molecular signals are obscured by the strong THz absorption of solvent water. Most reported THz biosensors require the tested samples to be tediously dried or replaced with a low-absorption medium, which impairs the original bioactivity and the distribution homogeneity of targets. As described in this proposed strategy, a molecule-specific THz biosensor was fabricated from an aptamer hydrogel-functionalized THz metamaterial. Benefitting from the strong interaction with the localized electric field of the metamaterial, trace thrombin-induced variations in the hydration state of the hydrogel can be sensitively probed, which was investigated experimentally and theoretically. The optimized THz biosensor exhibited remarkable specificity for actual serum sample assays and excellent sensitivity, with a relatively low detection limit of 0.40 pM in the human serum matrix. The proposed strategy could serve as a model system to develop various molecule-specific THz biosensors for aqueous molecule sensing.

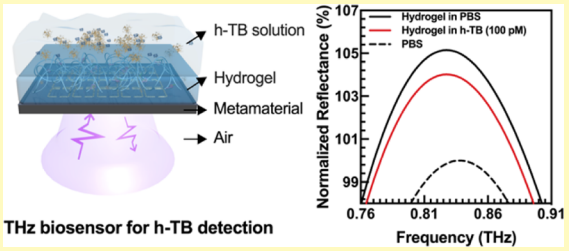

KEYWORDS: *terahertz metamaterial, aptamer hydrogel, terahertz biosensor, label-free sensing, aqueous molecule sensing*

Terahertz (THz) spectroscopy, a promising analytical method, can probe the coherent collective vibration modes of molecules in a label-free and nonionizing manner, carrying information on their structure and activity features.[1] Thus, this approach has been extensively utilized to identify solid molecules by their characteristic peaks and reveal the hydration dynamics of aqueous molecules from conformation-related hydrogen-bonding network changes,[2,3] demonstrating many unique advantages over other spectroscopic techniques. Although the quantitative measurement of pure aqueous molecules by THz spectroscopy has been reported in some strategies,[4,5] its sensing performance, including specificity and sensitivity, cannot fully meet the real-world requirements, especially for clinical analysis where the sample matrix often contains thousands of molecules. This shortcoming is because in aqueous environments, solvent water generates strong THz absorption (~240 cm^{-1} at 1 THz) and severely obscures the response of solute molecules, leading to similar absorption features (mostly from solvent water) for different trace aqueous molecules.[6] To weaken the interference of solvent water, most proposed THz biosensors require that the tested samples be tediously dried or that the solvent water be replaced with a low-absorption medium.[2,7,8]

Nevertheless, THz spectroscopy could obtain a limited absorption signal of tiny dried molecules due to the mismatch between the wavelengths of THz waves and the dimensions of molecules.[9] THz metamaterials, comprising subwavelength periodic artificial structures with obvious resonance peaks in the THz band, could greatly enhance the interactions between incident THz waves and adherent target molecules through an excited localized electric field.[6] Such metamaterials have been demonstrated to be a highly sensitive biosensing platform whose resonance frequency and peak intensity display profound alterations in a concentration-dependent manner, even for trace target molecules.[10] Hence, THz metamaterials have been employed for widespread practical implementation in sensing proteins,[9] nucleic acids,[11] cells[12] and other molecules[13] with high performance, and bioimaging.[14] In addition, molecule-specific THz metamaterials can be realized by decorating antibodies or aptamers on their interfaces or by using functionalized nanoparticles with a high refractive index.[15] However, drying processes are still indispensable in most THz metamaterial-based biosensors; these processes are harmful to the original biomolecular activity and affect the

Received: January 27, 2021
Accepted: April 29, 2021
Published: May 12, 2021

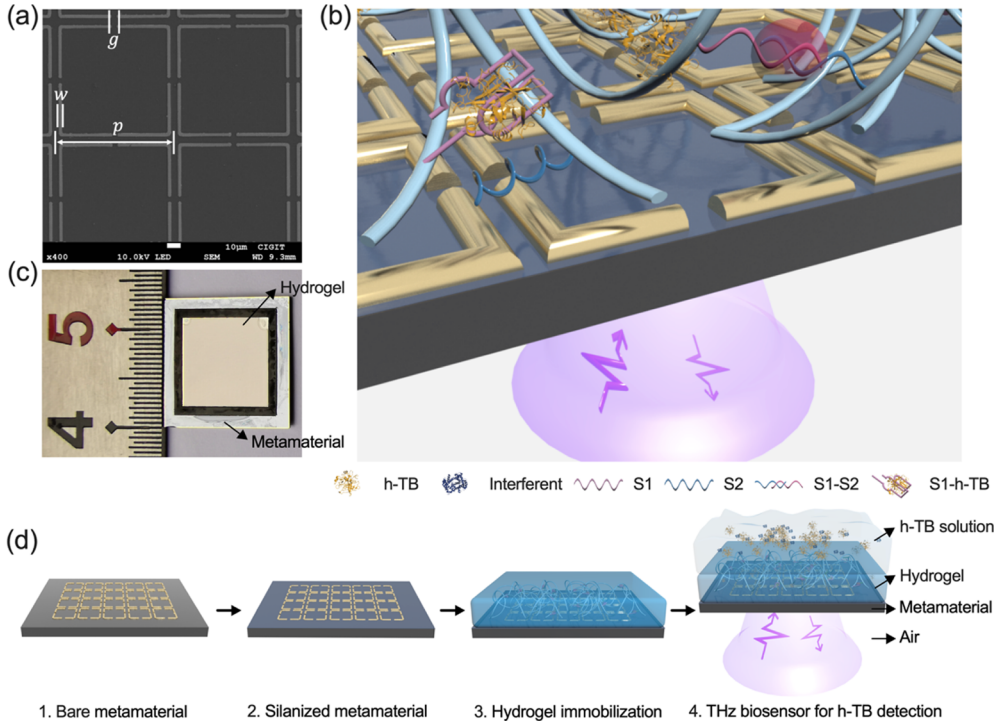

Figure 1. (a) SEM image of the bare THz metamaterial. (b) Schematic representation of h-TB sensing by the THz biosensor. (c) Physical image of the THz biosensor. (d) Experimental procedure of the proposed strategy.

homogeneity of the sample distribution (called the "coffee-ring effect").[2,16] Therefore, THz sensing strategies that work in aqueous environments are urgently needed for the direct, homogeneous, and *in situ* analysis of trace targets in the physiological state. To date, the strong absorption of water in the THz range has posed a considerable challenge to effectively unravel the mystery of aqueous molecules.[17,18]

Inspired by the very high THz absorption of water, our group has devoted great attention to aptamer hydrogels. Aptamer hydrogels are three-dimensional hydrophilic and insoluble polymeric networks grafted by aptamers that are extensively hydrated and sensitive to external stimuli; these networks have attained considerable interest in material-to-biology communication.[19] Owing to their high affinity for target molecules, aptamers endow hydrogels with the ability of highly specific molecular recognition.[20] Notably, the recognition process of target molecules considerably alters the crosslinking density of aptamer hydrogels, thus leading to profound variations in the volume and hydration state.[21] Furthermore, this binding reaction can enrich target molecules in the hydrogel matrix, bringing significant signal amplification.[19] Taken together, with water as a unique enhancer for THz measurements, aptamer hydrogel-functionalized THz metamaterials may sensitively reveal trace target-induced variations in the hydration state of hydrogels, which is promising for developing a molecule-specific THz biosensor applicable to aqueous environments.

Herein, for trace analysis of human α-thrombin (h-TB) in highly absorptive aqueous environments, a THz biosensor was constructed by *in situ* polymerization of an aptamer-grafted hydrogel film on a silanized metamaterial and was monitored in the self-referenced reflection measurement mode. The feasibility of the proposed THz biosensor was successfully verified by simulations and experiments. The performance of the optimized THz biosensor exhibited excellent sensitivity and satisfactory specificity for h-TB solution detection. Furthermore, the applicability of the THz biosensor was investigated by detecting h-TB in serum, showing great potential in clinical applications.

EXPERIMENTAL SECTION

Preparation of Functionalized THz Metamaterials. The THz metamaterial was fabricated by a standard photolithography technique. Metal evaporation of Cr/Au (20 nm/200 nm) was performed on a 500 μm thick high-resistivity silicon wafer (>10,000 Ω·cm). As shown in Figure 1a, the period (p), gap size (g), and width (w) of the unit cell are 70, 4, and 2 μm, respectively. The polydimethylsiloxane films with different thicknesses were bonded to the edge of the metamaterial to prepare the hydrogel with the corresponding swelling thickness. The bare metamaterial was cleaned sequentially with absolute ethanol and ultrapure water and dried with high-purity N_2. To enhance the adhesion of the hydrogel to the metamaterial, the cleaned metamaterial was activated by oxygen plasma for 5 min at 30 W with a pressure of 150 mTorr (Sindin, SPV10, China) and subsequently pretreated in (3-aminopropyl)-triethoxysilane (APTES)/absolute ethanol (1:9, v/v) solution for 24 h at 40 °C. Finally, the silanized metamaterial was rinsed with absolute ethanol and dried under high-purity N_2.

Immobilization of Aptamer Hydrogels. To prepare the aptamer hydrogel, a stock solution mixture of 100 μM aptamer (S1) and 100 μM complementary sequence (S2) was incubated at 65 °C for 5 min and then cooled to room temperature. The precursor solution was composed of a mixture of 15 μM S1, 15 μM S2, 10% (m/v) acrylamide (Am), 0.1% (m/v) *N*,*N*-methylene-bisacrylamide (MBAA), and 0.5% (m/v) ammonium persulfate. After degassing in a vacuum desiccator for 5 min, the precursor solution was dropped uniformly over the silanized THz metamaterial. 0.5% (v/v) *N*,*N*,*N*′,*N*′-tetramethylethylenediamine was quickly added and blended into the precursor solution. Then, a glass slide processed with Repel-Silane was immediately pressed on the surface of the THz metamaterial and kept there for approximately 30 min to complete the polymerization. The electrophoresis results verified the polymerization reaction, as shown in Figure S1. Finally, the glass slide was

https://doi.org/10.1021/acssensors.1c00174
ACS Sens. 2021, 6, 1884−1890

carefully peeled off, and the aptamer hydrogel-functionalized THz metamaterial was obtained. For the immobilization of the aptamer, a silanized metamaterial was immersed in the 5 μM aptamer solution for 2 h at 45 °C and then was rinsed with phosphate-buffered saline (PBS) to prepare the aptamer-functionalized THz metamaterial.

Preparation of Samples for THz Measurements. To optimize the appropriate THz measurement mode, the transmission and reflection spectra of the THz biosensor were compared (Figure S2); the results revealed that the resonance peak of the THz biosensor in the transmission measurement disappeared due to the severe attenuation of the solution.[17] Therefore, the THz biosensor was measured by a commercial THz-TDS system in the reflection mode (TAS7500SP, Advantest, Japan). Notably, a self-referenced method was introduced to simplify the operation and obtain stable data.[22] Pulse I (~15−22 ps) of the measured THz time-domain waveforms, which originated from the air−metamaterial interface, was taken as the reference signal, and pulse II (~29−36 ps), which was reflected from the metamaterial−hydrogel interface, served as the sample signal (Figure S3). After performing a fast Fourier transform, the self-referenced reflection signal of the THz biosensor was extracted by dividing the frequency amplitude of the sample signal by that of the reference signal.

Before THz measurements, swelling equilibrium of the hydrogel was achieved in PBS. The remaining solution on the metamaterial undersurface was completely removed, while sufficient solution was retained on the hydrogel surface (named the "upper solution"). The self-referenced reflection signal of the THz biosensor was recorded by THz spectroscopy. Then, the THz biosensor was incubated in the tested solution for 3 h while shaking at 200 rpm. Subsequently, the signal variation (ΔR) of the self-referenced resonant peak intensity of the THz biosensor was calculated by the equation $\Delta R = (R_c - R_s)/(R_c - R_0)$, where R_c, R_s, and R_0 refer to the measured resonant peak intensities of the THz biosensor before and after incubation in the tested solution and the bare THz metamaterial with individual PBS drops, respectively.

RESULTS AND DISCUSSION

Principle of the Molecule-Specific THz Biosensor. As shown in Figure 1, the THz biosensor consists of two main components: an h-TB-responsive aptamer hydrogel and an APTES-pretreated THz metamaterial. The aptamer (S1) and its complementary sequence (S2) are grafted onto the MBAA cross-linked linear polyacrylamide polymer to prepare an aptamer hydrogel containing a hydrophilic and insoluble porous network structure (Figure 1b).[23] Then, the aptamer hydrogel is tightly immobilized on the silanized THz metamaterial with a homogeneous structure to fabricate the proposed THz biosensor (Figure 1c). The self-referenced reflection measurement mode is exploited to read out the signal of the THz biosensor, as described in Figure 1d. In contrast to two-scan traditional transmission measurements, which require microfluidic channels to limit the thickness of the solution layer to <100 μm,[24] the proposed measurement mode achieves real-time and high-throughput extraction of hydrogel dielectric properties in one scan regardless of liquid thickness and the influence of laser turbulence.[22]

For the sensitive detection of h-TB, the metamaterial was introduced and strongly coupled with incident THz waves to excite THz spoof surface plasmons. The resonance behavior, equivalent to an LC resonance, provides a considerably enhanced electric field around the gap of the metal structure (Figure S4), increasing the sensitivity of analyte detection. The resonant frequency and intensity of the resonance peak are strongly associated with the refractive index and extinction coefficient of the equivalent dielectric environment of the resonator−analyte interface, respectively.[15] The THz absorption features of analytes (i.e., biomolecules, cells, and tissues) are lower than those of water molecules coming from the intermolecular vibrations of the hydrogen-bond network, allowing direct and sensitive determination of their hydration-state changes. Upon the introduction of h-TB, it preferentially binds with the grafted aptamer, leading to the breaking of the crosslinking points of S1−S2 and the further swelling of the hydrogel due to the decrease in the degree of effective crosslinking (molar ratio of S1−S2 to MBAA), thus altering the hydration state of the hydrogel.[25] This hydration-state shift affects the THz absorption features of the hydrogel (mainly reflected in the extinction coefficient), modifies the localized electric field, and alters the intensity of the measured resonance peak of the THz biosensor;[26] this process was investigated by FDTD numerical simulations (details in the Simulations section of the Supporting Information), and the results are described as follows.

Simulated Results of the THz Biosensor. The key to the proposed strategy is the preparation of a hydrogel with an appropriate thickness to effectively eliminate interference from the upper solution and determine the potential sensing performance of the THz biosensor. The extinction coefficient of the aptamer hydrogel, measured by THz-attenuated total reflection spectroscopy, was lower than that for PBS and showed an increase after incubation (Figure 2a). As shown in Figure 2b,c, the simulated resonance peak intensity of the THz biosensors increased as the thickness of the hydrogel increased from 0 to 10 μm and gradually became saturated as the thickness increased further and reached a maximum at 50 μm. In other words, the interference of the upper solution could be ignored with changes in the thickness of the hydrogel in an

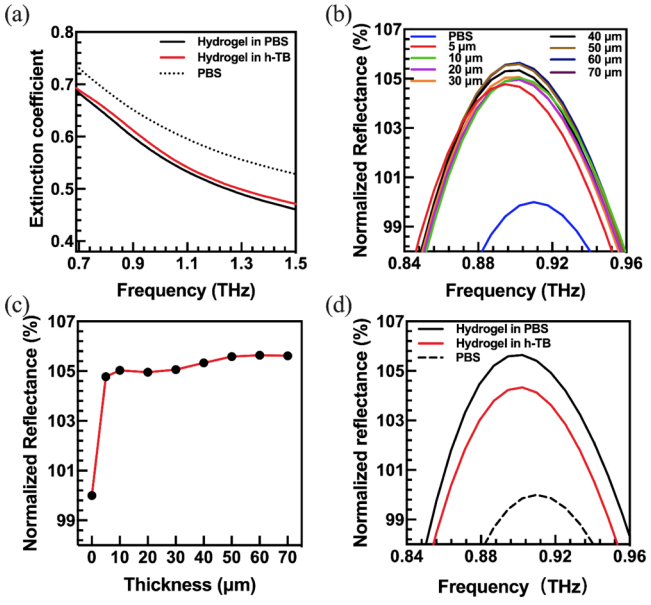

Figure 2. (a) Measured extinction coefficients of the PBS solution (black dotted line) and that of the swollen hydrogel before (black solid line) and after (red solid line) the induction of h-TB (100 pM). (b) Simulated self-referenced reflection spectra of the THz biosensor with swollen hydrogel thicknesses ranging from 0 to 70 μm. (c) Simulated resonance peak intensity of THz biosensors with swollen hydrogel thicknesses ranging from 0 to 70 μm. (d) Simulated self-referenced reflection spectra of the THz biosensor before (black solid line) and after (red solid line) the induction of h-TB (100 pM) and of the bare THz metamaterial with only PBS drops (black dotted line).

https://doi.org/10.1021/acssensors.1c00174
ACS Sens. 2021, 6, 1884−1890

appropriate range, which provides a basis for the optimization of the sensing system. We investigated the response to the extinction coefficient variation of the hydrogel, and the simulated resonance peak intensity was significantly reduced (~23.26%) after 100 pM h-TB was applied (Figure 2d), numerically validating the sensing mechanism of the proposed strategy described above. Therefore, the proposed THz biosensor is theoretically reasonable and feasible, which requires further experimental verification.

Feasibility of the Proposed Strategy. As expected, the resonance peak intensity of the functionalized THz biosensor was significantly higher than that of the bare metamaterial with only PBS added (Figure 3a). We compared the self-referenced

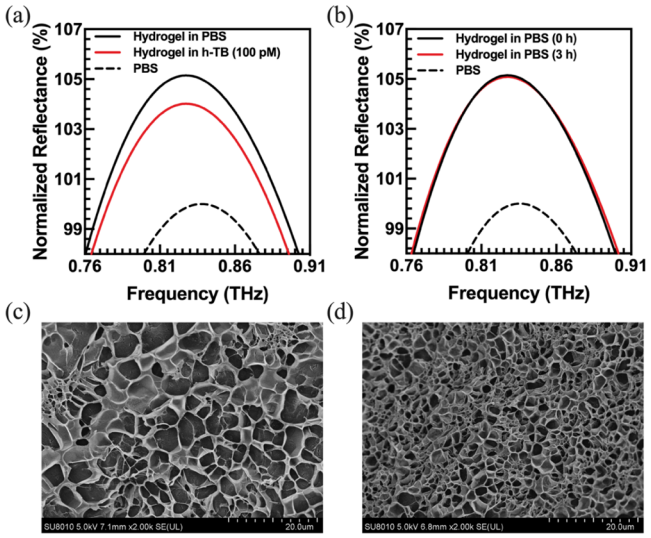

Figure 3. (a) THz spectra of the THz biosensor before (black solid line) and after (red solid line) the induction in h-TB (100 pM) and of the bare THz metamaterial with only PBS drops (black dotted line). (b) THz spectra of the THz biosensor incubating in PBS at 0 h (black solid line) and 3 h (red solid line) and of the bare THz metamaterial with only PBS drops (black dotted line). SEM images of the cross-sectional structure of the freeze-dried hydrogel after incubation in h-TB (100 pM) (c) and in PBS (3 h) (d).

reflection spectra of the THz biosensor after incubation in PBS with/without h-TB (100 pM), and the resonance peak intensity was markedly decreased after the application of h-TB, while no obvious changes were observed after exposure to PBS (Figure 3b). The calculated signal variations of the THz biosensor after exposure to h-TB and PBS were 22.19 and 1.32%, respectively, agreeing well with the simulation result (~23.26%). This finding strongly suggests that the aptamer hydrogel located in the effective sensing area may undergo a significant increase in the hydration state. In contrast, no significant differences were observed in the self-referenced reflection spectra of aqueous h-TB and interferents [including human hemoglobin (Hb), bovine thrombin (b-TB), and bovine serum albumin (BSA)] dropped on the bare metamaterial (Figure S5). These results further prove that the aptamer hydrogel, as an excellent sensing medium, clearly promotes the sensitive detection of h-TB in aqueous environments, which has rarely been achieved by individual metamaterials.

To explore the origin of the signal variation, the crosslinked network of the freeze-dried hydrogel was further characterized by scanning electron microscopy (SEM) (Figure 3c,d). The average pore size of the porous network structure inside the hydrogel increased significantly after the incubation in h-TB, confirming that the hydrogel indeed experienced a significant increase in the hydration state caused by the decreased crosslinking density after specifically capturing h-TB. In particular, the dissociation of crosslinking points S1−S2 caused by the binding reaction between S1 and h-TB may also induce an increasing dynamical hydration shell and the corresponding augmentation of the absorbance of the hydrogel.[3] Given that the degree of effective crosslinking of the hydrogel was calculated to be ~0.23%, the signal variation in the THz biosensor was not attributed simply to the decreasing crosslinking density. We anticipated that this variation may come from other considerations, including entropy theory, entanglement-excluded volume, or some weak interaction force change inside the hydrogel network, whose vibrational resonances were located in the THz range. These results further proved that THz spectroscopy is especially suitable for hydrogel-based sensing strategies from a new perspective, unlike other optical biosensors based on target-induced changes in the volume or refractive index of the hydrogel.[19,27]

Optimization of the Proposed Strategy. We further optimized several critical experimental parameters for high-performance sensing. Consistent with the above simulation results, Figure 4a shows that the signal variation of the THz

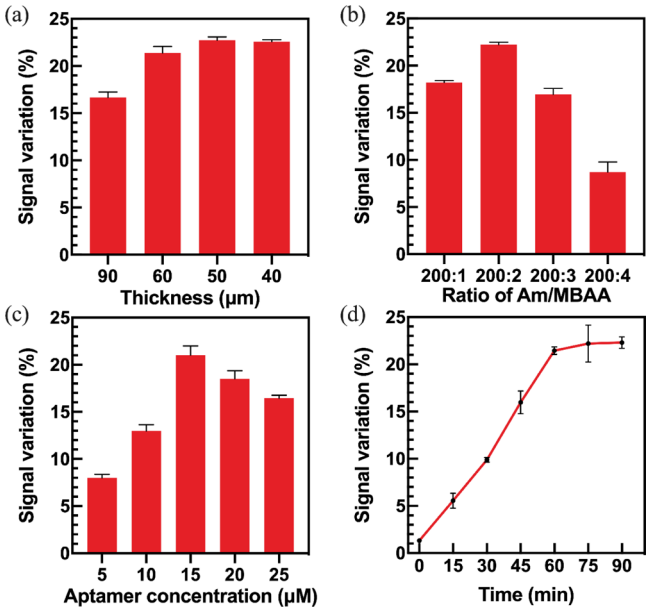

Figure 4. Optimization of critical experimental parameters. The concentration of h-TB is 100 pM. (a) Thickness of the hydrogel. (b) Crosslinking density (ratio of Am/MBAA) of the hydrogel. (c) Concentration of the aptamer in the precursor solution (aptamer/complementary sequence = 1:1). (d) Reaction kinetics of the THz biosensor in the h-TB solution. Error bars indicate standard deviations (n = 3).

biosensor gradually increases with decreasing hydrogel thickness, and the greatest signal variation is produced at 50 μm. According to the literature,[28] the crosslinking density and thickness of the hydrogel are critical for the sensitivity and response time. As shown in Figure 4b, the signal variation of THz biosensors with different crosslinking densities of the hydrogel, prepared by adjusting the MBAA content in the precursor solution, reaches the maximum at the ratio Am/

https://doi.org/10.1021/acssensors.1c00174
ACS Sens. 2021, 6, 1884−1890

MBAA = 200:2. As the crosslinking density continues to increase, the signal variation decreases rapidly. As is known, the dimensional selectivity of the polyacrylamide hydrogel was determined by different ratios of Am/MBAA so that different sizes of molecular sieves were formed. Therefore, the excessively high crosslinking density restricts the binding reaction of h-TB and aptamer and the swelling behavior of the hydrogel. Additionally, the concentration of the aptamer is important because it acts as the recognition element to specifically capture h-TB and thus effectively alters the crosslinking density. Figure 4c indicates that the most significant signal variation is observed in the THz biosensor with an aptamer concentration of 15 μM. Subsequently, according to the above optimized parameters, the reaction kinetics of the prepared THz biosensor were investigated (Figure 4d). The signal variation rapidly increases and nearly reaches a plateau after 60 min, which shows a significantly faster response speed benefiting from the thin hydrogel with an appropriate crosslinking density. As a model system, the proposed strategy could be tailored to respond to small molecules such as metal ions,[29] glucose,[30] and adenosine[31] within minutes by grafting other target-specific recognition moieties and has considerable potential for point-of-care test applications.

Performance of the Proposed Strategy. The sensing performance of the optimized THz biosensor was investigated for h-TB detection. As shown in Figure 5a, the signal variation of the THz biosensor increased gradually with increasing concentrations of h-TB and revealed linearity with the logarithm of h-TB concentration from 0.5 to 500 pM (R^2 = 0.9842). The limit of detection (LOD) is determined as 0.21 pM here (Inset), which achieves the self-referenced reflection signal variation that is higher than the blank signal plus 3 times its standard deviation. As a comparison, the aptamer-functionalized THz metamaterial was prepared without any hydrogel networks, similar to previous research,[24] but it can hardly discriminate PBS from aqueous h-TB (Figure 5b), which emphasizes the necessity of an aptamer hydrogel-functionalized strategy. In terms of sensitivity, the proposed THz biosensor also outperforms most label-free sensing strategies and is even comparable to labeled detection methods (Table S1). The excellent performance of the THz biosensor is primarily attributed to the enhanced THz-substance interaction of metamaterials, the strong THz absorption of water (serving as a super enhancer), the unique enrichment effect of hydrogels, and the strong affinity of aptamers for h-TB (dissociation constant k_d = 0.5 nM).[32] There are significant advantages in this strategy: (1) simplicity: only *in situ* polymerization of the precursor solution is required, without further binding and blocking operations; (2) stability: the hydrogel network can protect the grafted aptamers; and (3) high sensitivity: a target-induced change in the hydration state of the hydrogel could cause a profound relative dielectric constant change near the THz metamaterial rather than an individual aptamer−target binding reaction.

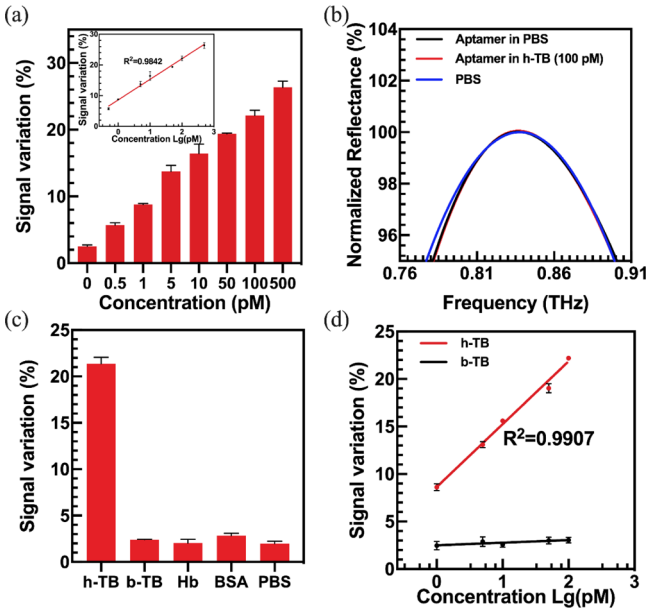

Figure 5. Sensing performance of the THz biosensor. (a) Sensitivity of the THz biosensor for the detection of h-TB in PBS ranging from 0.5 to 500 pM. (Inset) Linear relationship between the signal variation and the logarithm of h-TB concentration. (b) THz spectra of the aptamer-functionalized THz metamaterial before (black solid line) and after (red solid line) the induction in h-TB (100 pM) and of the bare THz metamaterial with only PBS drops (blue solid line). (c) Specificity evaluation of the THz biosensor for the detection of h-TB against interferents in PBS. (d) Quantitative analysis of h-TB and b-TB in serum samples. Error bars indicate standard deviations (n = 3).

The specificity of the proposed THz biosensor was investigated by comparing the signal variation of 100 pM h-TB, b-TB, Hb, and BSA, as shown in Figure 5c. The degree of interference (DI) was less than 5% (2.22% for b-TB, 0.34% for Hb, and 4.42% for BSA), calculated by the formula DI = $(\Delta R_I - \Delta R_0)/(\Delta R_T - \Delta R_0) \times 100\%$, where ΔR_I, ΔR_0, and ΔR_T represent the signal variation of the THz biosensor after incubation in the interference substance, PBS, and h-TB, respectively. As seen, these interferents induced only a slight signal variation ($P > 0.05$), consistent with previous results using aptamer hydrogel-functionalized diffraction gratings.[25] This is because the grafted aptamer could selectively recognize the target and prevent the interferent solution from effectively sensing the area occupied by the aptamer hydrogel. Without the need for any further tedious isolation and purification processes, the proposed method could achieve selective *in situ* analysis in aqueous environments.

Practical Sample Assay. Evaluating the sensing performance of the proposed strategy in complex matrices is indispensable for future clinical applications. Since commercially available human serum contains negligible h-TB and coagulation factors, the additional h-TB does not introduce errors in the experimental determination.[33] The quantitative assays of h-TB and b-TB in commercially available human serum were performed with three replicates. As shown in Figure 5d, the signal variation was proportionally increased to the logarithm of h-TB concentrations with an LOD of 0.40 pM, compared to the insignificant differences in b-TB analysis. The remarkable signal variation for serum sample analysis is indeed due to the high-specificity and high-affinity capture of h-TB by the aptamer, so common interferents such as b-TB could not break the crosslink points between the aptamer and the complementary sequence and generate obvious variations. Although the metamaterial design may be common, the proposed THz biosensor with excellent sensing performance exactly verifies the necessity and universality of introducing an aptamer hydrogel and demonstrates that such an approach could immediately confer any THz metamaterial the ability of

https://doi.org/10.1021/acssensors.1c00174
ACS Sens. 2021, 6, 1884−1890

specific and sensitive sensing in aqueous environments. We believe that further improvement of this biosensor by using a low-dielectric-constant substrate and a novel sensing mechanism (e.g., Fano resonance or the electromagnetically induced transparency effect) will boost the development of THz spectroscopy in more clinical applications.

CONCLUSIONS

In summary, a molecule-specific THz biosensor prepared from an h-TB-responsive aptamer hydrogel-functionalized metamaterial was successfully developed for the sensitive, label-free, and quantitative detection of h-TB in aqueous environments. Benefiting from the strong THz absorption of water and the enhanced localized electric field of the metamaterial, the proposed strategy displays an excellent sensing performance with an LOD of 0.40 pM in serum, far better than the aptamer-functionalized THz metamaterial. Notably, the THz biosensor demonstrates significant improvement in the detection specificity of THz spectroscopy for aqueous samples and even serum by virtue of the aptamer hydrogel. Thus, the proposed strategy, as a model system, brings to light new avenues for the development of molecule-specific THz biosensors suitable for point-of-care applications and clinical diagnosis.

ASSOCIATED CONTENT

Supporting Information

The Supporting Information is available free of charge at https://pubs.acs.org/doi/10.1021/acssensors.1c00174.

Characterization of the polymerization reaction; comparison of the transmission and reflection spectra of the THz biosensor; principle of self-referenced THz measurement; electric field distribution of the THz metamaterial; reflection spectra of aqueous h-TB and interferents; comparison of the proposed and reported strategies; and relative standard deviation of the data in the manuscript (PDF)

AUTHOR INFORMATION

Corresponding Authors

Xiang Zhao − *Department of Oncology, Southwest Hospital, Third Military Medical University (Army Medical University), Chongqing 400038, China*; Email: x.zhao.tmmu@outlook.com

Yunxia Wang − *Department of Laboratory Medicine, Southwest Hospital, Third Military Medical University (Army Medical University), Chongqing 400038, China*; Email: wyx_amu@126.com

Weiling Fu − *Department of Laboratory Medicine, Southwest Hospital, Third Military Medical University (Army Medical University), Chongqing 400038, China*; orcid.org/0000-0002-2695-6604; Email: weiling_fu@126.com

Authors

Jie Zhou − *Department of Laboratory Medicine, Southwest Hospital, Third Military Medical University (Army Medical University), Chongqing 400038, China*

Guorong Huang − *Department of Laboratory Medicine, Southwest Hospital, Third Military Medical University (Army Medical University), Chongqing 400038, China*

Xiang Yang − *Department of Laboratory Medicine, Southwest Hospital, Third Military Medical University (Army Medical University), Chongqing 400038, China*

Yang Zhang − *Department of Laboratory Medicine, Chongqing University Cancer Hospital, Chongqing 400038, China*

Xinyu Zhan − *Department of Laboratory Medicine, Southwest Hospital, Third Military Medical University (Army Medical University), Chongqing 400038, China*

Huiyan Tian − *Department of Laboratory Medicine, Southwest Hospital, Third Military Medical University (Army Medical University), Chongqing 400038, China*

Yu Xiong − *Department of Laboratory Medicine, Southwest Hospital, Third Military Medical University (Army Medical University), Chongqing 400038, China*

Complete contact information is available at: https://pubs.acs.org/10.1021/acssensors.1c00174

Author Contributions

‖J.Z. and X.Z. contributed equally.

Funding

This work was supported by the Military Logistics Scientific Research Project (AWS17J010), the National Natural Science Foundation of China (82002250), the Basic Science and Frontier Technology Research Project of Chong Qing (cstc2017jcyjBX0004), and the Chongqing Health Commission (2019ZDXM025).

Notes

The authors declare no competing financial interest.

REFERENCES

(1) Gil-Santos, E.; Ruz, J. J.; Malvar, O.; Favero, I.; Lemaître, A.; Kosaka, P. M.; García-López, S.; Calleja, M.; Tamayo, J. Optomechanical Detection of Vibration Modes of a Single Bacterium. *Nat. Nanotechnol.* **2020**, *15*, 469−474.

(2) Seo, M.; Park, H. R. Terahertz Biochemical Molecule-Specific Sensors. *Adv. Opt. Mater.* **2020**, *8*, 1900662.

(3) Nibali, V. C.; Havenith, M. New Insights into the Role of Water in Biological Function: Studying Solvated Biomolecules Using Terahertz Absorption Spectroscopy in Conjunction with Molecular Dynamics Simulations. *J. Am. Chem. Soc.* **2014**, *136*, 12800−12807.

(4) Morales-Hernández, J. A.; Singh, A. K.; Villanueva-Rodriguez, S. J.; Castro-Camus, E. Hydration Shells of Carbohydrate Polymers Studied by Calorimetry and Terahertz Spectroscopy. *Food Chem.* **2019**, *291*, 94−100.

(5) Zhao, X.; Zhang, M.; Wei, D.; Wang, Y.; Yan, S.; Liu, M.; Yang, X.; Yang, K.; Cui, H.-L.; Fu, W. Label-Free Sensing of the Binding State of MUC1 Peptide and Anti-MUC1 Aptamer Solution in Fluidic Chip by Terahertz Spectroscopy. *Biomed. Opt. Express* **2017**, *8*, 4427−4437.

(6) Lee, S.-H.; Shin, S.; Roh, Y.; Oh, S. J.; Lee, S. H.; Song, H. S.; Ryu, Y.-S.; Kim, Y. K.; Seo, M. Label-Free Brain Tissue Imaging using Large-Area Terahertz Metamaterials. *Biosens. Bioelectron.* **2020**, *170*, 112663.

(7) Yang, K.; Yang, X.; Zhao, X.; Lamy de la Chapelle, M.; Fu, W. THz Spectroscopy for a Rapid and Label-Free Cell Viability Assay in a Microfluidic Chip Based on an Optical Clearing Agent. *Anal. Chem.* **2019**, *91*, 785−791.

(8) Yang, K.; Li, J.; Lamy de la Chapelle, M.; Huang, G.; Wang, Y.; Zhang, J.; Xu, D.; Yao, J.; Yang, X.; Fu, W. A Terahertz Metamaterial Biosensor for Sensitive Detection of Micrornas Based on Gold-Nanoparticles and Strand Displacement Amplification. *Biosens. Bioelectron.* **2021**, *175*, 112874.

(9) Ahmadivand, A.; Gerislioglu, B.; Manickam, P.; Kaushik, A.; Bhansali, S.; Nair, M.; Pala, N. Rapid Detection of Infectious

Envelope Proteins by Magnetoplasmonic Toroidal Metasensors. *ACS Sens.* **2017**, *2*, 1359−1368.
(10) Xu, W.; Huang, Y.; Zhou, R.; Wang, Q.; Yin, J.; Kono, J.; Ping, J.; Xie, L.; Ying, Y. Metamaterial-Free Flexible Graphene-Enabled Terahertz Sensors for Pesticide Detection at Bio-Interface. *ACS Appl. Mater. Interfaces* **2020**, *12*, 44281−44287.
(11) Lee, S.-H.; Choe, J.-H.; Kim, C.; Bae, S.; Kim, J.-S.; Park, Q.-H.; Seo, M. Graphene Assisted Terahertz Metamaterials for Sensitive Bio-Sensing. *Sens. Actuators, B* **2020**, *310*, 127841.
(12) Yan, X.; Yang, M.; Zhang, Z.; Liang, L.; Wei, D.; Wang, M.; Zhang, M.; Wang, T.; Liu, L.; Xie, J.; Yao, J. The Terahertz Electromagnetically Induced Transparency-Like Metamaterials for Sensitive Biosensors in the Detection of Cancer Cells. *Biosens. Bioelectron.* **2019**, *126*, 485−492.
(13) Wang, Y.; Cui, Z.; Zhang, X.; Zhang, X.; Zhu, Y.; Chen, S.; Hu, H. Excitation of Surface Plasmon Resonance on Multiwalled Carbon Nanotube Metasurfaces for Pesticide Sensors. *ACS Appl. Mater. Interfaces* **2020**, *12*, 52082−52088.
(14) Ma, Q.; Cui, T. J. Information Metamaterials: bridging the physical world and digital world. *PhotoniX* **2020**, *1*, 1.
(15) Xu, W.; Xie, L.; Zhu, J.; Xu, X.; Ye, Z.; Wang, C.; Ma, Y.; Ying, Y. Gold Nanoparticle-Based Terahertz Metamaterial Sensors: Mechanisms and Applications. *ACS Photonics* **2016**, *3*, 2308−2314.
(16) Lee, S. H.; Lee, D.; Choi, M. H.; Son, J. H.; Seo, M. Highly Sensitive and Selective Detection of Steroid Hormones Using Terahertz Molecule-Specific Sensors. *Anal. Chem.* **2019**, *91*, 6844−6849.
(17) Lee, D.-K.; Yang, H.; Song, H. S.; Park, B.; Hur, E.-M.; Kim, J. H.; Park, T. H.; Seo, M. Ultrasensitive Terahertz Molecule Sensor for Observation of Photoinduced Conformational Change in Rhodopsin-Nanovesicles. *Sens. Actuators, B* **2018**, *273*, 1371−1375.
(18) Yang, X.; Zhao, X.; Yang, K.; Liu, Y.; Liu, Y.; Fu, W.; Luo, Y. Biomedical Applications of Terahertz Spectroscopy and Imaging. *Trends Biotechnol.* **2016**, *34*, 810−824.
(19) Bai, W.; Gariano, N. A.; Spivak, D. A. Macromolecular Amplification of Binding Response in Superaptamer Hydrogels. *J. Am. Chem. Soc.* **2013**, *135*, 6977−6984.
(20) Dhanjai; Sinha, A.; Kalambate, P. K.; Mugo, S. M.; Kamau, P.; Chen, J.; Jain, R. Polymer Hydrogel Interfaces in Electrochemical Sensing Strategies: A Review. *TrAC, Trends Anal. Chem.* **2019**, *118*, 488−501.
(21) Elsherif, M.; Hassan, M. U.; Yetisen, A. K.; Butt, H. Glucose Sensing with Phenylboronic Acid Functionalized Hydrogel-Based Optical Diffusers. *ACS Nano* **2018**, *12*, 2283−2291.
(22) Wu, X.; Pan, X.; Quan, B.; Xu, X.; Gu, C.; Wang, L. Self-Referenced Sensing Based on Terahertz Metamaterial for Aqueous Solutions. *Appl. Phys. Lett.* **2013**, *102*, 151109.
(23) Lin, Z.-T.; Li, Y.; Gu, J.; Wang, H.; Zhu, Z.; Hong, X.; Zhang, Z.; Lu, Q.; Qiu, J.; Wang, X.; Bao, J.; Wu, T. A Conductive Nanowire-Mesh Biosensor for Ultrasensitive Detection of Serum C-Reactive Protein in Melanoma. *Adv. Funct. Mater.* **2018**, *28*, 1802482.
(24) Shih, K.; Pitchappa, P.; Jin, L.; Chen, C.-H.; Singh, R.; Lee, C. Nanofluidic Terahertz Metasensor for Sensing in Aqueous Environment. *Appl. Phys. Lett.* **2018**, *113*, 071105.
(25) Wang, X.; Wang, X. Aptamer-Functionalized Hydrogel Diffraction Gratings for the Human Thrombin Detection. *Chem. Commun.* **2013**, *49*, 5957−5959.
(26) Miyamaru, F.; Hattori, K.; Shiraga, K.; Kawashima, S.; Suga, S.; Nishida, T.; Takeda, M. W.; Ogawa, Y. Highly Sensitive Terahertz Sensing of Glycerol-Water Mixtures with Metamaterials. *J. Infrared, Millimeter, Terahertz Waves* **2013**, *35*, 198−207.
(27) Peng, L.; You, M.; Yuan, Q.; Wu, C.; Han, D.; Chen, Y.; Zhong, Z.; Xue, J.; Tan, W. Macroscopic Volume Change of Dynamic Hydrogels Induced by Reversible DNA Hybridization. *J. Am. Chem. Soc.* **2012**, *134*, 12302−12307.
(28) Dautta, M.; Alshetaiwi, M.; Escobar, J.; Tseng, P. Passive and Wireless, Implantable Glucose Sensing with Phenylboronic Acid Hydrogel-Interlayer RF Resonators. *Biosens. Bioelectron.* **2020**, *151*, 112004.
(29) Huang, Y.; Fang, L.; Zhu, Z.; Ma, Y.; Zhou, L.; Chen, X.; Xu, D.; Yang, C. Design and Synthesis of Target-Responsive Hydrogel for Portable Visual Quantitative Detection of Uranium with a Microfluidic Distance-Based Readout Device. *Biosens. Bioelectron.* **2016**, *85*, 496−502.
(30) Zhang, X.; Guan, Y.; Zhang, Y. Ultrathin Hydrogel Films for Rapid Optical Biosensing. *Biomacromolecules* **2012**, *13*, 92−97.
(31) García-Astrain, C.; Lenzi, E.; de Aberasturi, D. J.; Henriksen-Lacey, M.; Binelli, M. R.; Liz-Marzán, L. M. 3D-Printed Biocompatible Scaffolds with Built-In Nanoplasmonic Sensors. *Adv. Funct. Mater.* **2020**, *30*, 2005407.
(32) Tasset, D. M.; Kubik, M. F.; Steiner, W. Oligonucleotide Inhibitors of Human Thrombin that Bind Distinct Epitopes. *J. Mol. Biol.* **1997**, *272*, 688−698.
(33) Zhang, L.; Lei, J.; Liu, L.; Li, C.; Ju, H. Self-Assembled DNA Hydrogel as Switchable Material for Aptamer-Based Fluorescent Detection of Protein. *Anal. Chem.* **2013**, *85*, 11077−11082.

https://doi.org/10.1021/acssensors.1c00174
ACS Sens. 2021, 6, 1884−1890